Influence of isotopic substitution and He coimplantation on defect complexes and voids induced by H ions in silicon

O. Moutanabbir* and B. Terreault
INRS-EMT, Université du Québec, 1650 Boulevard Lionel-Boulet, Varennes, Québec, Canada J3X 1S2

M. Chicoine and F. Schiettekatte
Département de physique, Université de Montréal, Montréal, Québec, Canada H3T 1J4

P. J. Simpson
Department of Physics and Astronomy, University of Western Ontario, London, Ontario, Canada N6A 3K7
(Received 22 August 2006; published 1 February 2007)

We present a detailed study of the comparative thermal evolutions of H- and D-related defects in silicon implanted with 2×10^{16} H or D/cm^2, or coimplanted with 0.25×10^{16} He/cm^2 and 0.7×10^{16} H/cm^2, in both orders. By using ion channeling, positron annihilation spectroscopy, and Raman scattering spectroscopy, we found that hydrogen and deuterium interact remarkably differently with primary point defects. He post implantation is found to destroy vacancies highly passivated by hydrogen, whereas He preimplantation accelerates their evolution into atomically smooth internal surfaces. By comparing different systems, subtle points in the interactions between the implanted atoms and point defects are evidenced, and critical defect complexes involved in silicon blistering are identified. Finally, the origins of the isotopic and synergistic effects observed in low energy ion-induced silicon blistering are discussed.

DOI: 10.1103/PhysRevB.75.075201 PACS number(s): 61.72.Qq, 61.82.Fk, 61.80.Lj

I. INTRODUCTION

Hydrogen-related effects play an important role in semiconductor physics and technology. The subject has been reviewed several times over the years (Pearton *et al.*,[1] Myers *et al.*,[2] Cerofolini *et al.*,[3,4] Van de Walle,[5] Estreicher,[6] and Jones *et al.*[7]). In particular, hydrogen is known to passivate dangling or defective bonds. In the bulk, this serves to remove undesirable levels in the band gap; on the surface, it is used to protect against oxidation in preparation for various processing steps such as thin film deposition; and at the Si-SiO_2 interface it ensures a defect-free frontier. Hydrogen also forms complexes with impurities, including intentionally introduced dopants, and can deactivate their electrical activity, with positive or negative consequences depending on the case. Finally, H-ion implantation, and also He-ion implantation, can produce gas-filled cavities. These have two applications: one is the gettering of unwanted heavy metal impurities, the second is "ion cutting," which, together with wafer bonding, is used in silicon-on-insulator fabrication and other heterogeneous integration processes. One of the principal methods of introducing hydrogen in solids is ion implantation, which unavoidably produces radiation damage. Understanding the evolution of hydrogen and helium irradiation induced defects is thus vital in order to be able to control the processes cited above.

The present work is concerned with hydrogen blistering of silicon,[8,9] in relation to the technology based on this phenomenon, ion cutting.[10] Blistering is known to occur in a large variety of semiconductors, silicon being the prototypical one. It may take place either as a result of high dose implantation (over 10^{17} H/cm^2) at room temperature (RT), or following thermal annealing of wafers implanted with more moderate ion doses, e.g., a few 10^{16} H/cm^2. It is the last case we are interested in. Moreover, we have focused on blistering by low-keV ions, as the trend to miniaturization inevitably leads to implantation at shallower depths using lower energy ions. Exploring the limits of a phenomenon may also lead to new effects.

The study of the thermal evolution of defects has clarified several major points in relation to blistering.[3,4,8,9,11–20] (Rather than reviewing these works here, it will be easier to cite them in connection with the different points in our discussion.) In spite of all this work, new phenomena remain to be discovered or explained. For instance, in order to single out the contribution of defects, isotope substitution has been used in the study of blistering, based on the fact that deuterons produce more than twice as many Frenkel defects as protons (the exact numbers depend on the ion energy). Large differences were indeed found between H- and D-ion-induced blistering: D-induced blistering, unexpectedly, requires two to three times higher ion doses than H blistering.[21] Another intriguing effect is that implantation of a tiny dose of He ions prior to H-ion implantation allows blistering at much lower total ion doses.[22–27]

A first detailed study of the comparative evolutions of H- and D-related defects was carried out by looking at the Si-H/D stretch modes using Raman scattering spectroscopy (RSS).[28] This technique is strictly sensitive to those defects which are passivated by H/D atom attachment to dangling bonds. In the present paper, we report further studies using (1) Rutherford backscattering in the channeling mode (RBS/C) and (2) positron annihilation spectroscopy (PAS). The first of these techniques detects lattice atoms displaced away from their crystalline sites.[29] It is therefore very sensitive to interstitial defects but much less so to vacancies; lattice distortions can also give rise to a significant RBS/C signal, which will turn out to be important here. For its part,

TABLE I. Mean projected range R_p, range standard deviation ΔR_p, peak ion concentration (normalized to 10^{16} ion/cm^2) $C_{\max}$, depth of peak energy deposition into recoils R_d, peak value of energy deposition into recoils (normalized to 10^{16} ion/cm^2) $E_{d\,\max}$, and vacancies per ion, calculated by the code SRIM2003 (Ref. 31).

Parameter	Ion		
	H (5 keV)	D (5 keV)	He (8 keV)
R_p (nm)	76	92	90
ΔR_p (nm)	29	37	39
$C_{\max}$ for 10^{16} ion/cm^2 (at. %)	3.2	2.1	2.0
R_d (nm)	50	67	64
$E_{d\,\max}$ for 10^{16} ion/cm^2 (eV/atom)	4.0	9.6	43
Vacancies per ion	6.8	19.5	78.5

PAS (Ref. 30) is sensitive to regions of low electron density, i.e., voids in the lattice, whether they be vacancies or larger structures such as *platelets*[11] and bubbles; it is therefore quite complementary to RBS/C. In order for the paper to be self-contained and for the comparison to be complete, some of the main RSS results will also be recalled.

II. EXPERIMENTAL DETAILS

Cz-grown *n*-type (001) Si wafers (1–10 ohm cm resistivity) were cut into 1 cm^2 pieces and ultrasonically cleaned with solvents. Many identical samples were implanted at RT and normal incidence with either 2×10^{16} H/cm^2 or 2×10^{16} D/cm^2, both at 5 keV, or else successively implanted with 0.25×10^{16} He/cm^2 at 8 keV and 0.7×10^{16} H/cm^2 at 5 keV, in both orders. The samples did not significantly heat up during implantation since the beam power was only $\sim$10 mW/cm^2. The base pressure of the implanter is $<10^{-7}$ mbar. In Table I we show relevant implantation parameters calculated using the SRIM code,[31] i.e., implant depth, straggling and peak concentration, and radiation damage depth and intensity. It is seen that while the ion ranges do not differ strongly, on the other hand the primary defect production rates of D ions and He ions are respectively 2.8 and 11.5 times that of H ions. Although channeling of implanted ions is practically unavoidable at these low implantation energies,[32] it was checked that implantation at 15° tilt angle had in fact no effect on the results.

The important points for the present study are the following. (i) The H-implanted samples blistered after annealing at >450 °C, whereas the D-implanted samples did not, at any temperature: a dose of $\sim6\times10^{16}$ D/cm^2 is required for full blistering.[21] This isotope effect is "robust" in the sense that it prevails whatever the heating rate (from 0.3 to 300 K/s), in high resistivity Si as well as in low resistivity heavily Sb-doped or B-doped Si,[33] and with He+H/D coimplantation.[27] (ii) The samples implanted with He first and H second did blister, while the samples implanted in the reverse order did not, even for total ion doses up to 3×10^{16} at/cm^2.[27] This confirms Ref. 25 for the case where the He is implanted deeper than the H; note, however, that we have a strong overlap between our H and He depth distributions, when the widths of the profiles are taken into account (Table I).

RBS/C in the ⟨001⟩ axial channeling mode was performed using a 2 MeV He$^+$ beam on the Tandetron accelerator at the Université de Montréal. The channeling direction was found with a precision better than 0.1° by interpolating between planar channeling directions. The incident beam was defined by a ∅2 mm aperture. The typical beam current was 5 nA. Each time, the current on the target was confirmed by a current measurement in a Faraday cup. The outgoing particles were detected at 170° by a movable passivated implanted planar silicon (PIPS) detector with ~15 keV energy resolution. The sample-detector distance and detection solid angle were 122 mm and 6.7 msr, respectively. The resulting depth resolution is ~40 nm. A number of samples, as implanted or annealed in N_2 at different temperatures, were analyzed (after cooldown). The annealing protocol consisted of a linear ramp of 0.33 K/s up to the target temperature, in the range 200–600 °C, and an immediate shutoff of the heat source.

Similarly annealed samples were analyzed by PAS at the University of Western Ontario positron facility. PAS uses a beam of monoenergetic positrons (e^+) to probe open volumes in a solid target. Prior to positron analysis, samples were HF etched to remove the surface oxide, which can mask near-surface defects. Positron energies in the range 0.5 to 30 keV were used, to probe a range of depths in the samples from near-surface to ~4 microns. The e^+ energy-depth relation is not linear and the depth resolution is limited both by the straggling in e^+ slowing down and by its diffusion afterwards, and it varies from tens of nm at the surface to hundreds of nm deeper. Spectra containing 10^6 events were collected and analyzed using the conventional S (or "sharpness") parameter. The positron beam current is in the femtoampere range, and the technique is nondestructive.

Raman scattering analyzes were accomplished with a Renishaw 3000 system having a resolution of 2 cm^{-1}. The excitation was supplied by an Ar-ion laser (514.5 nm, 25 mW) at normal incidence. The laser light was focused on the sample surface through a 50× objective lens, and the diameter of the focused laser spot was about 3 μm. The scattered light was collected at RT by a CCD detector (collection time: 500 s, averaging factor: 4), and the background luminescence was subtracted from the data. The samples were subjected to a linear ramp of 0.33 K/s up to, e.g., 200 °C, allowed to cool to RT for measurement, and then ramped up again to a higher temperature, and so on. The RSS spectra are all normalized with respect to the data at RT.

III. EXPERIMENTAL RESULTS

A. Rutherford backscattering/channeling

In Fig. 1 are shown the backscattering spectra from the H-implanted samples, either after RT implantation, or after annealing at the indicated temperatures. The signals obtained from a nonimplanted (virgin) sample and that obtained with a nonchanneled (random) incident He$^+$ beam are also shown.

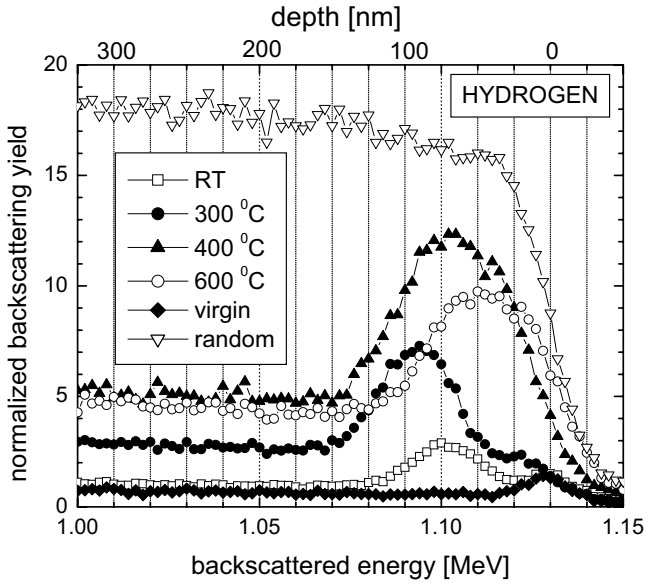

FIG. 1. Energy spectra of He^+ backscattered from different hydrogen implanted and annealed Si(001) samples, with the incident beam channeled in the ⟨001⟩ direction. The spectra of virgin samples, one in channeling conditions and the other in a random direction are also shown. An approximate depth scale is indicated as the top abscissa. The data are normalized to the same He^+ ion fluence.

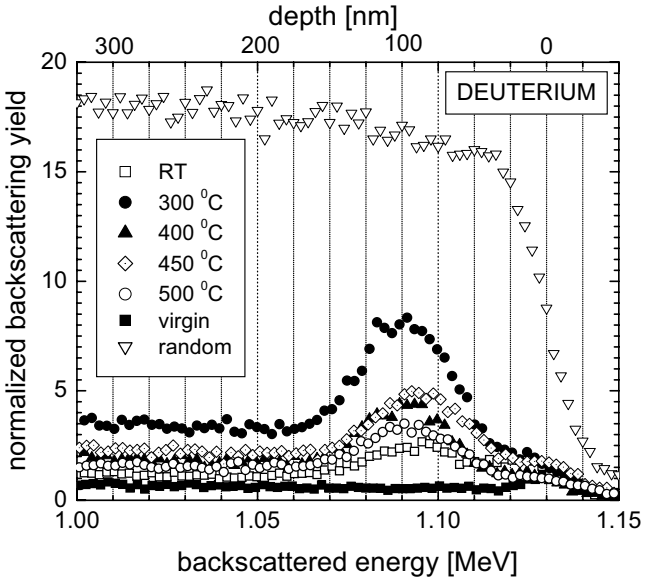

FIG. 2. RBS/C yields as a function of annealing temperature for deuterium-implanted Si(001) substrates.

All the data are normalized to the same He^+ beam fluence. The ratio between the virgin and random data is an indication of the quality of the crystals and the precision of the alignment. The small peak at ~1.13 MeV in the virgin spectrum is due to backscattering on surface atoms. The top abscissa shows an approximate depth scale (the calculation of an exact depth scale requires an iterative procedure since the channeled and dechanneled parts of the beam suffer different energy losses). The data for the implanted samples show basically two features. The first is a peak roughly centered around the mean H-ion range (~75 nm, see Table I). Its classic interpretation would be that it reflects the location of the interstitial defects. However, the height of this peak increases after heating at 300 °C and even more so at 400 °C, contrary to the normal effect of annealing; it does not decrease appreciably until 600 °C, well above the blistering temperature (~475 °C). This *reverse annealing* has been observed from the very beginning in H-implanted Si.[3,8,9,16–18] Since heating can hardly create new self-interstitials, this effect shows that some other type of defect is involved. Such an atomic displacement field can in fact be due to a strong localized deformation of the lattice[4] and not only to interstitials and clusters. One can also note that the location of the peak moves under annealing: from ~75 nm at RT, it moves deeper to ~90 nm at 300 °C, back to ~70 nm at 400 °C and finally to ~40 nm at 600 °C. This suggests that the peak shuttles between the damage peak R_d and the concentration peak R_p (Table I; we remind the reader that our depth scale is approximate). The same back and forth motion was also observed by Cerofolini *et al.*[3] The second feature in the spectra is an enhancement in backscattering yield above the virgin level beyond the implanted zone (>150 nm). This is called dechanneling and it is due to the He^+ particles that have been scattered out of the channel and behave as random ions for the rest of their trajectories. Dechanneling saturates at 400 °C. The same kind of defect that has given rise to the direct backscattering can cause dechanneling as well.

Figure 2 now shows the similar spectra for D implantation. We see that the differences in blistering behaviors are reflected in the RBS/C spectra. First, we note that, at RT already, the peak yield for D is not anything like ~2–3 times higher than the peak yield for H, as would be expected from the defect creation rates of Table I, it is actually slightly lower. This indicates again that it is not directly connected with the self-interstitials but that it is intimately linked to the H or D atoms, which have comparable peak concentrations, with H having in fact the highest one (Table I). The thermal evolution is similar for H and D up to 300 °C but diverges remarkably afterwards. For D, the process literally aborts above 300 °C – and there is no blistering. Both peak and dechanneling yields decrease beyond 300 °C. The back and forth motion of the peak is also less perceptible; in particular, the shallow peak, seen at the highest temperature with H, is absent here. The RBS/C data alone give no hint as to the cause of this bifurcation.

The coimplantation results of Figs. 3 and 4 are equally instructive. With He first (Fig. 3), at RT as well as at 200 °C, the damage level is extremely low. A part of the explanation is of course that the doses are small: (0.25 He+0.7 H) $\times 10^{16}/\text{cm}^2$. But He ions should cause a large amount of damage, and if we just "scaled" the data using Table I, we should get a peak value approaching the random level in this case. The well-known explanation of this unexpected behavior is that He ion implantation actually leaves very few Frenkel defects in Si,[4] because these defects are mobile at RT and so easily recombine or disappear at sinks; in contrast, an appreciable fraction of the H-induced defects are captured and stabilized by the formation of H-Si bonds. Even so, the ratio of the RBS/C yield for He+H to that for H alone is

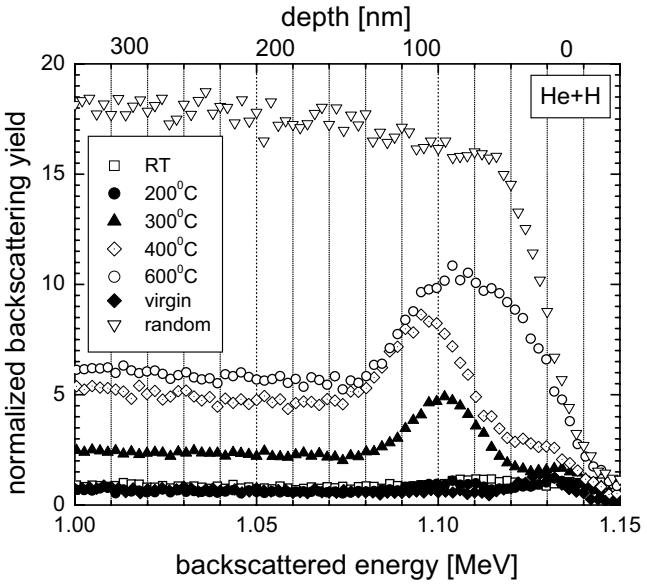

FIG. 3. RBS/C yields as a function of annealing temperature for Si(001) substrates coimplanted with He, then H (0.25×10^{16} He/cm^2+0.7×10^{16} H/cm^2).

negligible ($<1/10$) compared to the ratio of H doses (0.7/2). This shows that damage buildup is not linear with dose,[3] but also suggests that preimplanted He has an influence on the amount and type of damage that the H implantation produces. Nevertheless, the effect of He preimplantation is spectacular: the RBS/C yield rises continuously up to 600 °C and the sample blisters at very low total dose. The likely reason is that He is captured by the cavities that are the blister precursors and pressurizes them: Chabal *et al.*[15] and Lagahé-Blanchard *et al.*[25] showed how deeply implanted He migrates to the H-implanted region in the blistering process. Helium is a particularly effective pressurizer since it is gaseous at any temperature, contrary to H which remains chemisorbed up to 400–500 °C, and moreover has a single atom per molecule. The shuttle motion of the peak is also visible, and at 600 °C in particular, the shallow peak is clearly present. The last has also been seen in coimplantation by Tonini *et al.*[24] and attributed to the macroscopic lattice deformation of the blister caps. This interpretation is reinforced by our results since we see the shallow peak with H implantation also.

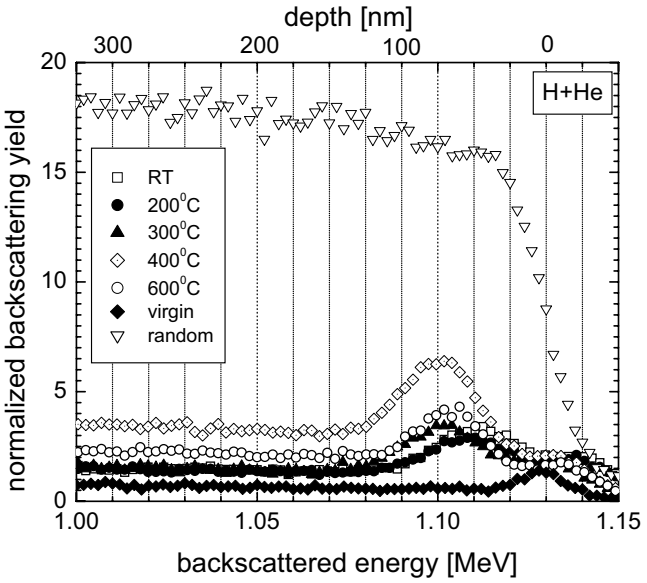

FIG. 4. RBS/C yields as a function of annealing temperature for Si(001) substrates coimplanted with H, then He (0.7×10^{16} H/cm^2+0.25×10^{16} He/cm^2).

Less straightforward is the explanation for the totally different behavior when He is implanted last (Fig. 4). Here, in spite of what we just stated about the ineffectiveness of He for permanent damage creation, the damage level at RT (and 200 °C) is paradoxically the same for 0.7×10^{16} H/cm^2 as for 2×10^{16} H/cm^2 alone. The difference is that the He is not implanted in virgin material but in one where H implantation has already created certain defect structures. We conjecture that some of these structures act as nuclei for the capture and stabilization of point defects generated during the subsequent He irradiation. But, contrary to the case of He first, annealing does not produce a very large increase in the peak and dechanneling yields: above 400 °C the yields drop to low values, there is no blistering, and there is no shallow peak at the highest temperature. This behavior suggests that the relatively high peak observed at RT with He last is due, in this case (and in this case only), not to H-related defects but to the "classic" interstitials and their clusters.

B. Positron annihilation spectroscopy

In PAS, the line shape of the γ ray is determined by the electron momentum distribution. In regions distant from atomic nuclei, such as vacancies or voids, the line has no high momentum tail. The S parameter measures the "sharpness" of the line, so it takes higher values in vacancies and cavities. By varying the incident positron energy, its penetration depth is changed, and a depth profile of cavities can be deconvoluted. Figure 5 shows our hydrogen data. At high energy, the expected well-known value for virgin Si is obtained. In the implanted region (~100 nm) an enhancement is observed, indicating the presence of cavities. The "open volume" increases up to 350 °C, dips slightly at 400 °C, and increases again up to 550 °C. Maxima at intermediate temperature (425 or 450 °C) were also seen in Ref. 3. This complicated behavior can result from adsorption and desorption in the cavities because PAS is not blind to the presence of H/D atoms in the cavities. The data of Uedono *et al.*[34] suggest that H passivation will reduce the S value of a cavity by ~0.0075 (1.5%). This is similar to the magnitude of the observed jumps. The peak S value obtained at 550 °C is ~1.05 times larger than the value for "bulk" silicon, which imposes a lower limit on the size of the positron trapping defects of at least four vacancies; for comparison the silicon divacancy yields an S parameter of 1.045 times the bulk silicon value.[35] However it is likely that the positron trapping defect is larger than V_4, since the measured value of $S=1.05$ represents a weighted average of trapped and untrapped positrons. These large voids are vacancy clusters, including *platelets*, which are flat cavities lying in low index atomic planes such as

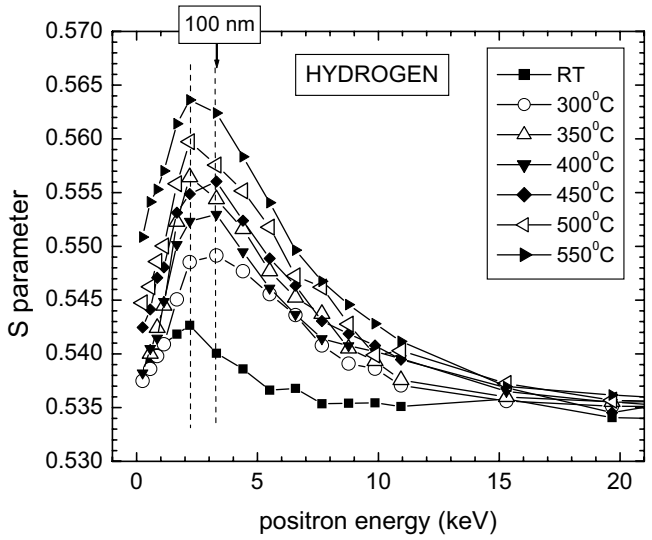

FIG. 5. Evolution of the S parameter profiles (S vs e^+ energy), as a function of annealing temperature, for Si(001) implanted with 2×10^{16} H/cm^2; an indication of the depth scale is given.

{100}, and of course blisters. Contrary to adsorbed atomic H, it seems that H_2 does not affect the S parameter much.[34] Another feature of interest is that the depth of the peak shifts in a way similar to the RBS/C peaks. At 300 °C it is deeper than at RT, then it moves towards the surface at 350 °C (when S has a maximum), then deeper again at 400–450 °C, and finally back towards the surface at 500–550 °C. This may seem erratic but the "shallow peak" is always associated with higher S values. In Ref. 3, the average void depth only increased with temperature, without shifting towards the surface.

Figure 6 shows the D data. The S value is generally lower than for H, consistent with the failure to evolve towards blistering. However, a strong and intriguing maximum in the D value is observed at 425–475 °C, reaching 1.06 times the

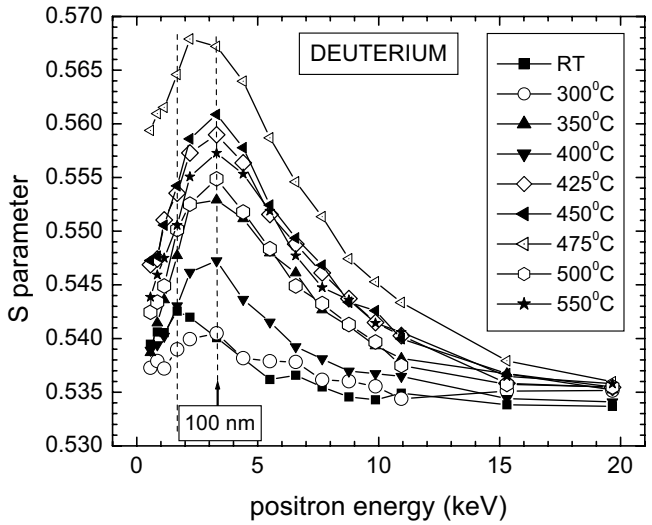

FIG. 6. Evolution of the S parameter profiles (S vs e^+ energy), as a function of annealing temperature, for Si(001) implanted with 2×10^{16} D/cm^2; an indication of the depth scale is given.

bulk value at 475 °C. Note that 475 °C (in addition to being the blistering temperature with H implants) is the only one, for D, for which there is a shift towards the surface; at and above 500 °C, the peak returns to the "deep" value. As in the case of H-implants, the shallow peak for S is thus associated with the highest S values and not necessarily the highest temperature. Supposing that the shallow peak in S, similar to the shallow peak in backscattering, is connected with blistering, it implies that large empty cavities did form at 475 °C but did not quite blister the surface, and flattened out at 500 °C.

Some PAS measurements were also made on H and D samples during a very slow anneal ($\sim10^{-2}$ K/s). In that case (not shown), the S-parameter for H was always larger than for D but neither sample was blistered at the end. This indicates that H blistering requires a minimum temperature ramping rate, whose value is larger than 10^{-2} K/s. The inhibition of blistering may be due to gas loss, because effusion has slow kinetics but is compensated by a small activation energy.

C. Raman scattering spectroscopy

The evidence of previous work[2–4,15] is that the major part of the H ions implanted in Si are trapped by defects. Due to the variety of defect configurations, the Si-H local vibrational stretch modes have a broad spectrum of wave numbers, k, in the range between ~1800 to ~2300 cm^{-1};[15] the corresponding k values for D atoms are scaled down by a factor of 1.39 as expected from the square root of the effective masses ratio. The identification of particular features in the spectra with specific defects is complicated; our assignments based on the literature are discussed in an earlier paper.[28]

In Fig. 7, a comparison of the Raman spectra for H- and D-implanted Si is given for four particularly critical temperatures.[28] It can be seen that an enormous difference between the Si-H and Si-D data is manifest at RT already. This difference therefore arises during the implantation: D atoms somehow interact in a different way than H atoms with the defects that are being continuously created. The D spectrum is bunched at low k values, which is characteristic of lightly passivated multivacancies V_nD_m, with $m\leq n$, and interstitial defects such as ID_2. In contrast, the H spectrum has a balance of low-k and high-k modes; the latter are due to saturated or almost saturated single or double vacancies ($VH_{3,4}$, V_2H_6), and also to passivated internal surfaces such as Si(001):H. It is generally assumed[15,28] that these internal surfaces are the same as the platelets observed by electron microscopy.[11,13,14] Since these platelets thus contain adsorbed hydrogen, in addition to being flat and parallel to the surface, they are naturally considered by most authors to be the blister precursors. A few other minor peaks are visible, but play no major role here; more details are found in Ref. 28. This difference in H vs D can be understood by comparing the defect production rates during implantation: D produces ~2.8 times more vacancies per implanted ion than does H, so we should expect to see a higher proportion of "saturated" vacancies for H than for D. The differences be-

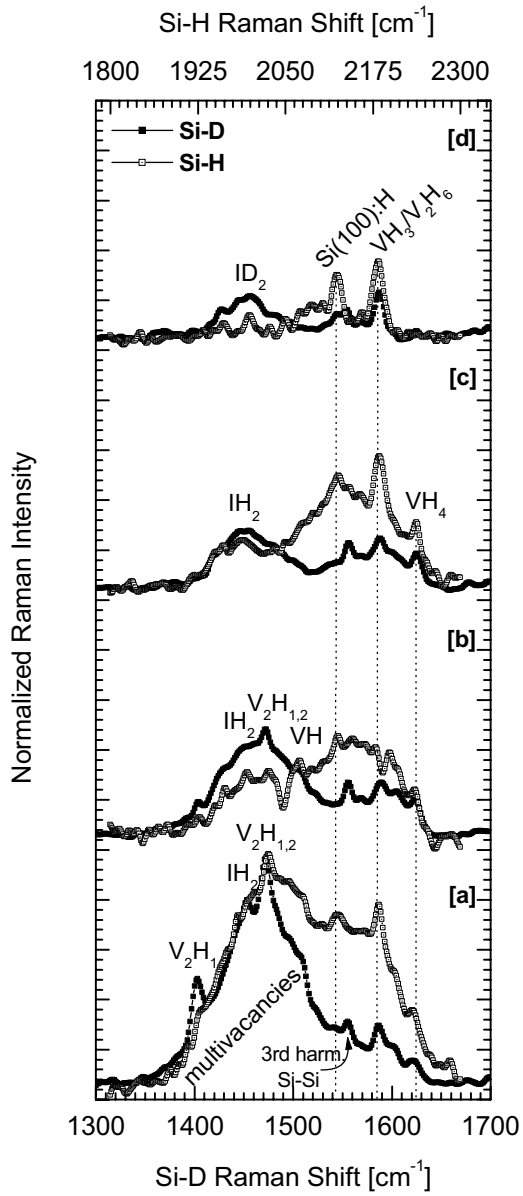

FIG. 7. Raman spectra in the Si-H (□) and Si-D (■) stretch region for several annealing temperatures: as implanted (a), 300 °C (b), 400 °C (c), 500 °C (d). Since the Si-D vibration frequencies are shifted down by a factor of 1.39 with respect to the Si-H ones, the wave number scales (top and bottom abscissas) have been carefully adjusted to make the corresponding Si-H and Si-D modes coincide.

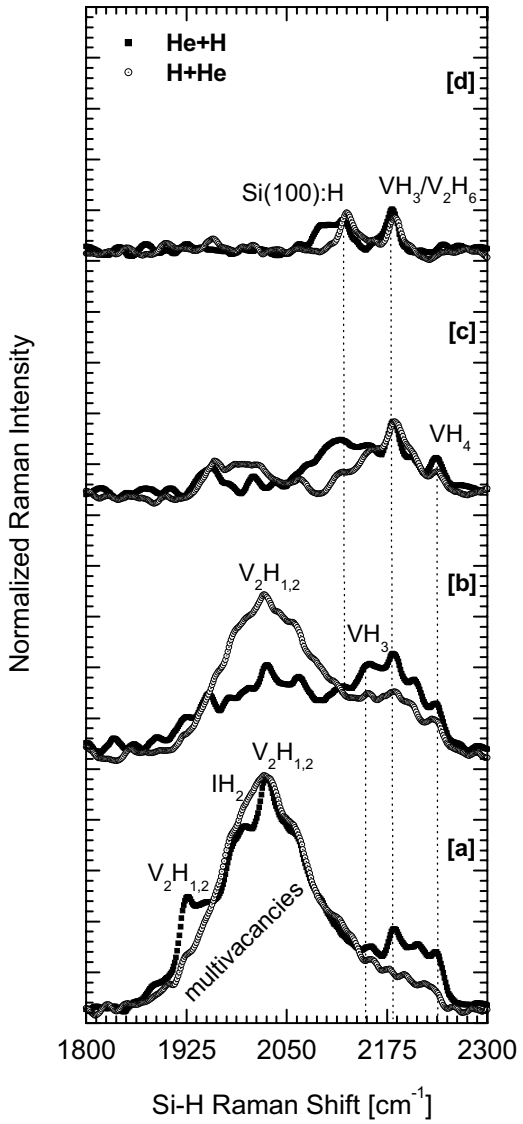

FIG. 8. Raman spectra in the Si-H stretch region for coimplanted samples for several annealing temperatures: as implanted (a), 300 °C (b), 400 °C (c), 550 °C (d); He implanted first (■), He implanted last (○).

come even more apparent after annealing [Figs. 7(b)–7(d)]. We recall that the spectra have been normalized with respect to the ones at RT. At 300 °C, while, for H, the low-k modes are strongly attenuated and the high-k modes clearly dominate, for D, the low-k modes are still the strongest. The higher stability of the V_nD_m compared to the V_nH_m suggests that they are made up of larger clusters, consistent with the higher Frenkel defect generation rate (Table I). At 400 °C, the VH_3 and/or V_2H_6 modes at ~2180 cm^{-1} (which are indistinguishable) appear to have actually increased. During that time, the D sample has evolved only moderately. Finally, at 500 °C, which is above the blistering temperature (for H only), the H spectrum is entirely dominated by the Si(100):H, and also by the VH_3/V_2H_6. The VD_3 and/or V_2D_6 have also finally emerged to some extent but not Si(100):D. Another difference is the persistence of the low-k modes for D.

Now we turn to coimplantation (Fig. 8).[27] At RT, one can immediately see the effect of He post implantation; these He ions were implanted in an already H-implanted sample that had a Raman spectrum similar to that of Fig. 7(a). All the narrow lines have been literally destroyed by the passage of the He ions. The same observation was made by Lagahé-Blanchard *et al.*[25] Moreover, the same group further found amorphous pockets by TEM.[26] On the contrary, with He preimplantation, the lines and in particular the saturated vacancies are still present. However, the high-k modes are not as strong as with H alone. This confirms that the presence of He influences the distribution of the bound H between different

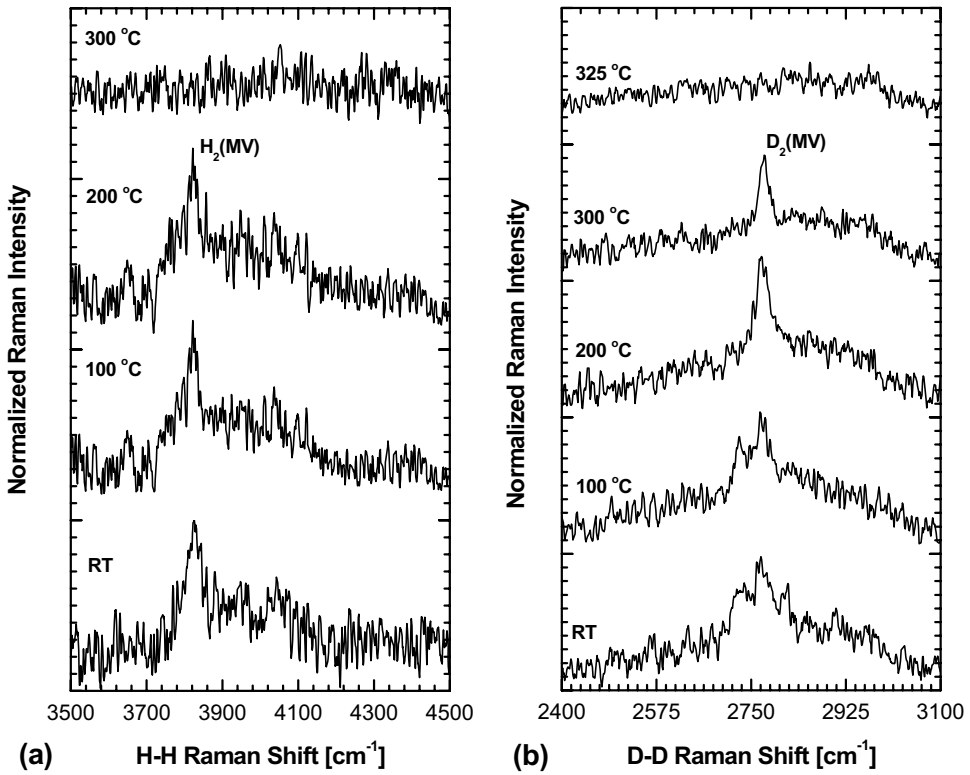

FIG. 9. Raman spectra of the H_2 and D_2 molecular stretch modes as a function of annealing temperature for silicon substrates implanted with: (a) 2×10^{16} H/cm^2; (b) 2×10^{16} D/cm^2.

types of defects. In spite of this fact, at 300 °C, the "He first" sample has already caught up with the "H alone" sample. At that temperature, the He last sample is still almost featureless. At 400 °C, the He damage has annealed in good part because both samples have evolved considerably. However, the decorated internal surfaces, Si(100):H, are well developed for He first, whereas they are still not apparent for H first. Finally, at 550 °C, the only large difference is the probably significant fact that the Si(100):H peak has a shoulder on the low-k side for He first, which is the sign of smoother and less defective surfaces:[15] We may suppose that this planarity helps in the propagation of cracks between adjacent platelets. It has also been shown theoretically[36] that a highly disordered Si lattice, as with He last, becomes more plastic and more resistant to crack propagation, possibly inhibiting blistering. The high temperature data of Ref. 25 differ in details, probably due to the nonoverlap between their He and H profiles, but the temperature evolution shows the same trends.

Raman scattering can also detect H_2 molecules (although the sensitivity is low). Indeed, we saw that the Si-H modes, especially the low-k ones, start disappearing progressively somewhere below 300 °C, while the total H contents measured by SIMS, ion-beam analysis or thermal desorption spectrometry remains almost constant up to ~450 °C. The H missing at intermediate temperature has consequently been assumed to be in the form of H_2.[3,4,11] Two molecular modes are already well known, gaseous H_2 at 4158 cm^{-1}, and H_2 in the interstitial T_d site at 3601 cm^{-1}.[37,38] We show in Fig. 9(a) our (hitherto unpublished) data in the 3500–4500 cm^{-1} spectral range. Neither $H_2(T_d)$ nor gaseous H_2 are detectable at our level of sensitivity. $H_2(T_d)$ has never been seen in implanted Si, only in plasma hydrogenated Si,[37] likely because there are stronger traps such as vacancies in implanted Si.[3] Free gaseous H_2 has been detected by Aspar *et al.*[13] only when they focused their exciting laser microbeam precisely on blisters (and after adding 50 spectra), but never outside blisters or at low or intermediate temperature. On the other hand we see in Fig. 9(a) a broad peak at ~3820 cm^{-1},[39,40] which has been attributed to H_2 in multivacancies, H_2(MV), such as V_2, V_6, and V_{10}.[39] We see that it disappears above 200 °C, in agreement with Ref. 39, and consistent with the disappearance of the multivacancy defects in the Si-H Raman modes (Fig. 7). Therefore it has nothing to do, at least directly, with the H_2 that pressurizes the blisters that appear at higher temperature. We also observe the corresponding D_2 mode around 2730–2815 cm^{-1}, which shows three resolved subpeaks [Fig. 9(b)]. Peak splitting is not observed in float-zone substrates,[39] and seems to be peculiar to the interactions of hydrogen (or deuterium) molecules with some defects in Cz silicon, thus suggesting that oxygen impurities might be a constituent of the complex. Each subpeak displays its own thermal behavior: the mode at 2815 cm^{-1} anneals out at 100 °C, the one at 2730 cm^{-1} at 200 °C, and the central one (2770 cm^{-1}) at 335 °C only. This shows that they are connected with different defects. The higher annealing temperature for the 2770 cm^{-1} mode compared to the 3820 cm^{-1} mode indicates a higher stability of the D-related multivacancy defects, in agreement with the Si-H/D data.

To summarize the Raman results, a strong presence at RT of the saturated (or near saturated) single or double vacan-

cies, and of high wave number modes ($k > 2050\ \mathrm{cm}^{-1}$) in general, is a predictor of eventual blistering. Under annealing, the low-k modes disappear while two narrow lines corresponding to VH_3 or V_2H_6 and Si(100):H rise above a fading background, and above 450 °C blisters start to deform the surface. The low-k modes tend to persist at high temperature whenever there is no blistering, be it with deuterium or with He post irradiation. There is no evidence for the H_2 molecules expected at intermediate temperatures: we call this the mystery of the *elusive hydrogen*.

IV. DISCUSSION

In order to characterize the RBS/C spectra in a simple way we define the normalized peak yield

$$NPY = \frac{Y_{\max} - Y_V}{Y_R - Y_V}, \tag{1}$$

where $Y_{\max}$ is the maximum value of the He^+ yield, Y_V and Y_R the virgin and random yields at the corresponding energy (or depth), respectively. Similarly, the normalized dechanneling yield is

$$NDY = \frac{Y_{dech} - Y'_V}{Y'_R - Y'_V}, \tag{2}$$

where Y_{dech} is the He^+ yield in the region beyond the implanted zone; Y'_V and Y'_R are the corresponding virgin and random yields, respectively. Calculations of *NDY* were performed by fitting the RBS/C spectra in the region 1.0–1.05 MeV; the yields were estimated from the fitted spectra at the arbitrarily chosen energy value of 1 MeV. For *NPY*, we used a Gaussian fit in a narrow region around the peak. Similarly we define $S_{\max}$ at a given temperature as the value of S at the peak in Figs. 5 and 6. With the help of these parameters we can summarize the thermal evolutions of the samples implanted with H or D or coimplanted with He and H. This is done in Fig. 10(a) for the normalized peak yield, in Fig. 10(b) for the normalized dechanneling yield, and Fig. 10(c) for the S parameter. Another phenomenon of interest is the occurrence of shifts in the depth profiles of displacement damage or void volume. These are summarized in Table II. We will constantly refer to Fig. 10 and Table II in the following discussions. The Raman data, on the other hand, are not so easy to summarize.

We note that the *NDY* data follow the same qualitative trends as the *NPY* data as a function of temperature, isotope, and order of implantation. The overall comparison suggests that the same features are responsible for both the displacement field in the implantation region and the enhancement in dechanneling beyond that region. These features are closely related to the H/D concentration rather than the point defects (except at RT, for He post implantation). Even without the evidence from deuterium, the comparison with He had led others[3] to conclude that their RBS yield in H-implanted Si was too large to be due to point defects. The reverse annealing behavior points to the same conclusion. However, between 300 and 400 °C, a critical point is reached where the outcome depends sensitively on the isotope or on the coimplantation order. Either the peak backscattering yield keeps increasing at the same time as it moves in and out in depth, and the sample blisters, or else *NPY* regresses and no blistering occurs.

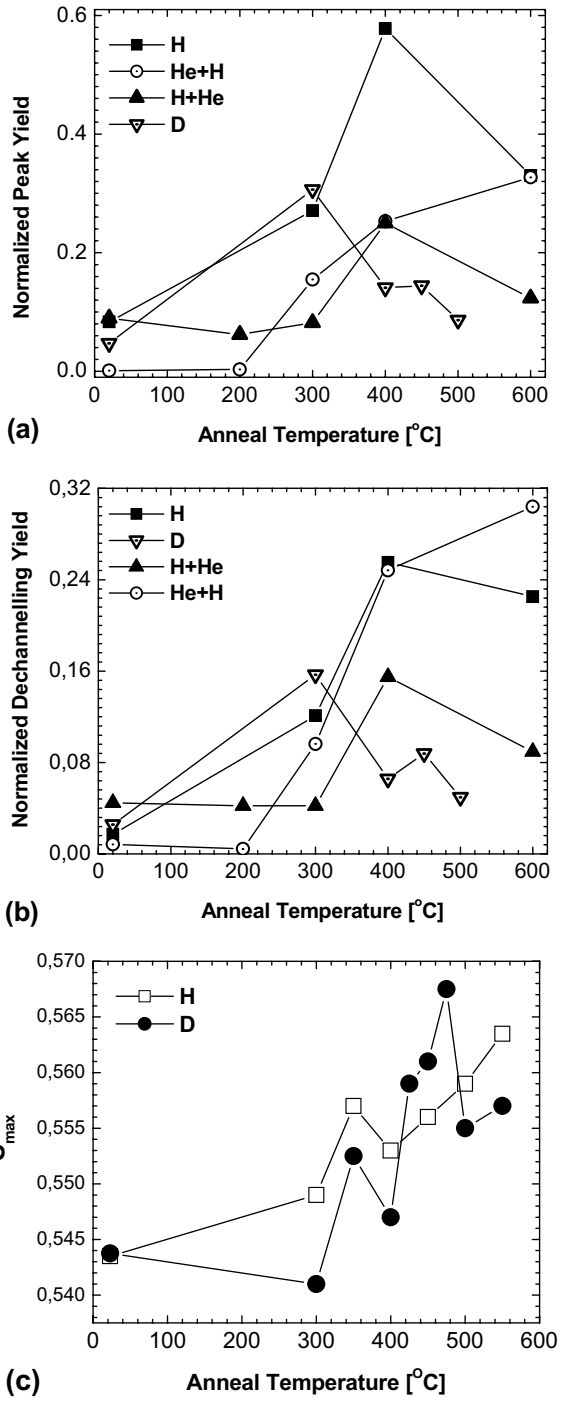

FIG. 10. Variations as a function of annealing temperature of: (a) normalized peak yields; (b) normalized dechanneling yields; and (c) the maximum S value, for the whole set of samples.

A candidate for the source of displacements and dechanneling could be thought to be the platelets, which are the largest defects and are clearly seen by TEM. In H-implanted Si (001), the most abundant are the (001) platelets, parallel to the surface.[11,13,14] Their diameter is on the order of 10 nm at

TABLE II. Temperatures of occurrence of shifts in depths of peak values of RBS/C yield or void volume measured by PAS (*S* parameter).

Quantity	Temperature range	
	Shift in depth	Strong shift to surface
RBS peak yield - H	300 °C	600 °C
S-parameter peak - H	300–450 °C	500–550 °C
RBS yield - D	300 °C	none
S-parameter peak - D	300–450 °C+500–550 °C	475 °C
RBS peak yield - He+H	400 °C	600 °C
RBS peak yield - H+He	300 °C	none

RT and thickness 1 nm. Their presence is also witnessed by the Si(100):H peak in the Raman spectrum. However, vacancies or cavities by themselves do not cause any backscattering or dechanneling, except indirectly through the tensile strain that they may induce. But the platelets actually display very little strain contrast in TEM and their internal surfaces appear remarkably undisturbed,[13] which makes them less likely to be at the source of the displacement field. Moreover, under annealing they grow in diameter at constant total volume, consistent with *Ostwald ripening*:[14] this should have the effect of further reducing the elastic strain, contrary to the RBS/C yield which springs to very high values at 300–400 °C. True, at still higher temperature, the platelets must fill with gaseous H_2 and coalesce catastrophically by pressure-driven crack propagation, causing blistering. That high pressure will cause a large strain–and this, indeed, is what is observed at 600 °C (Fig. 1), together with the shift towards the surface in the RBS/C peak. However, the initial rise in RBS/C definitely takes place long before that phase, and whatever H_2 the platelets may have contained, if we interpreted the signal in Fig. 9 as H_2 in platelets, disappears at 300 °C instead of accumulating. Besides, all the evidence indicates that the 3820/2760 cm^{-1} mode belongs to H_2/D_2 in multivacancies. One may then think of those multivacancies as the source of pressure and strain. However, as in the case of the platelets, this hypothesis is ruled out by their annealing behavior.

As a matter of fact, it is precisely when the multivacancies disappear (Figs. 7 and 8) that the RBS/C signals rise (Fig. 10). Indeed the magnitude of the RBS/C enhancement is positively correlated with the magnitude of the reduction in intensity of the low-*k* modes. This has led to two hypotheses. The first was that the H atoms and molecules liberated by the multivacancies were captured by the platelets as H_2.[15] However, we just saw that the platelets do not appear to contain gaseous H_2 at this stage; that H would then have to exist in some undetermined temporary form until the final stage at higher temperature. The other hypothesis,[3] based mainly on RBS/C and strain measurements, was that H_2, assumed to already exist as interstitial $H_2(T_d)$ at low temperature, was captured as gaseous H_2 by "small vacancy clusters" (especially V_4) above 200 °C. Cerofolini *et al.*[3] went further and proposed that these H_2-saturated "nanobubbles" were the blister precursors, rather than the platelets. A similar doubt as to the role of the platelets was also stated recently.[40] It is true that the final transformation of platelets into blisters has never been "visualized" because it is presumably too fast (<2 s and probably much less[41]) but the same is true for the coalescence of nanobubbles. However, the IR data of Ref. 15 and that of Figs. 7 and 8 show only VH_3/V_2H_6 and Si(100):H as the "survivors" of the rearrangements taking place at 300–400 °C. The "larger cavities" ($>V_4$) seen by PAS only show up at ~475–500 °C and their shift towards the surface together with the shift in the RBS/C profile identifies them with the blisters. It thus seems that the H liberated at intermediate temperature must be stored in a form undetectable by RSS until it is captured by the blister precursors at higher temperature. That unidentified form would also be responsible for the enhancement in backscattering and dechanneling, presumably through an induced strain. Stress or strain measurements have been reported by several authors but only two of them at temperatures higher than RT. Unfortunately the answer is ambiguous: the first[42] reports an *increase* at 300 °C, the second[43] a *decrease* at 350 °C, but the dose was high in the last case so that it is not clear if the blistering temperature had not been reached. Finally, it is interesting to note that the survival of the VH_3/V_2H_6 complexes at the blistering stage makes them plausible alternatives to the platelets as blister precursors, in a variant of the Cerofolini scenario. However, the very geometry and size of the platelets, and the ease of crack propagation in such a geometry, makes the platelets appear as the likely "culprits."

The strongest indication of H/D differences that appears at RT is in the Raman spectra, but it is of utmost importance since it determines the course of events under the subsequent annealing. How can H and D atoms react differently with the point defects produced during the implantation? Vacancy production rates predicted by SRIM are 6.8 per H ion, and 19.5 per D ion. However we expect that only 5–10 % of the vacancies formed will survive, since many recombine during implantation,[44] and this is not modeled by SRIM. If we assume that, e.g., 10% of the vacancies survive after implantation, then our H-implanted samples will have more H than *V*, and our D-implanted samples, more *V* than D. The process is actually amenable to theoretical calculations by the kinetic Monte Carlo method,[45] and preliminary results confirm semiquantitatively our data.[46] A different situation arises when He is post implanted. In that case, the RT RBS yield is six times larger than when He is preimplanted. It is also roughly the

same as with a three times bigger H dose alone. Let us make the assumption that the point defects generated by the He ion collisions are captured in this case, instead of annihilating. If we take into account the He dose (0.25×10^{16} cm^{-2}), it is seen that the post-irradiated He ions generate 12 times more RBS yield per ion than H ions. This is more in line with the relative energy deposition rates (Table I) and it indicates that the RBS yield is due to interstitial defects in this case. This is consistent with the Raman spectrum: we note that it is devoid of sharp peaks, an indication of heavy disorder of the multivacancy and interstitial cluster type. The likely dominant mechanism is vacancy capture by small vacancy clusters: this has the effect of both generating larger clusters and diluting the H in these clusters, in agreement with Raman spectra.

Only minor changes occur up to a temperature somewhere above 200 °C, but at 300 °C the evolution in RBS/C and Raman data is remarkable as already noted. The multivacancies, which, with their large open spaces, could have been thought of as natural precursors to blisters, on the contrary are useless because they do not contain enough chemisorbed H/D and are not flat either. The PAS signal has not yet changed too much in intensity; this may be because: (i) the total platelet cavity volume has not changed (Ostwald ripening), and moreover H-saturated vacancies give a reduced S value compared to empty cavities; (ii) interstitials would decrease S, if anything; and (iii) multivacancies are on the decline. However, the PAS maximum is now located deeper, indicating a shift in the void volume from multivacancies (peaking around R_d) to the platelets (R_p) or to the postulated "Raman-invisible" H-storing complexes responsible for the RBS/C signal increase.

There is another major turning point between 300 °C and 400 °C. In contrast to H, for D the RBS yield has now decreased and, consistently, Si(100):D has not yet emerged, although $V\mathrm{D}_3/V_2\mathrm{D}_6$ has. For He post irradiation Si(100):H is still not very strong but the RBS yield has finally increased. The S parameter has started to increase at 350 °C, which may indicate an increase in cavity volume; its fallback at 400 °C can be rationalized by the final collapse of the multivacancies and/or a capture of H by cavities.

In the cases where there is to be blistering, the final steps take place somewhere between 400 and 500 °C. For H, the only significant H-related complexes that remain at 500 °C are Si(100):H and $V\mathrm{H}_3/V_2\mathrm{H}_6$. There is some difference in the RBS/C yields depending on whether there was He preimplantation or not. For H alone, the trend is slightly downward, which could be due to a relaxation of the lattice strain resulting from a loss of some H_2 and gas pressure upon blistering.[21] With He, the RBS/C yield keeps increasing; this may be correlated with the fact that the He preimplant has the effect of retarding the effusion of H and He to higher temperatures: this is seen by both elastic recoil detection analysis of retention[23] and thermal desorption spectroscopy.[27] For instance, preimplanted He is only released in the range 700–900 °C, compared to 500–700 °C for post implanted He and 400–600 °C for H_2. Finally, the S-parameter increases rapidly, in perfect accord with the growth of the blisters.

Contrary to the scenario just described, with D, the Si(100):D are barely detectable even at 500 °C and, correspondingly, the RBS yield is back down already at 400 °C. The large enhancement in the S parameter which takes place between 425 and 475 °C is correlated with a shift towards the surface. If surface shifts indicate blistering or at least tentative blistering as postulated above, failure to blister may be caused by lack of pressure. A lower atom content than with H is suggested by the high S value, together with the low RBS/C signal. This may be a consequence of the greater rate of vacancy production for D vs H: the greater number of vacancies leads to void formation, but without sufficient gas available to stabilize the voids against annealing to higher temperatures. Whereas the smaller quantity of voids formed in H-implanted samples, with more gas available "per void," survive to lead to eventual blistering. Formation and subsequent breakup of multivacancies is ruled out by the Raman data, which shows a monotonic decrease in multivacancies with increasing anneal temperature. With He postimplantation, the situation is not as drastic, the RBS/C yield is somewhat higher than with D and the Si(100):H clearly appear at 550 °C, but apparently too late for blistering, a significant fraction of the gas has already been released.

V. CONCLUSION

We presented a detailed study of the thermal evolution of H-related defects leading to blistering and exfoliation of crystalline silicon. By combining Rutherford backscattering, positron annihilation and Raman scattering, we studied different critical defect complexes and identified their subtle transformations leading to blistering. Our analysis suggests that "free" hydrogen liberated from multivacancies plays the key role in strain buildup, which is manifested by the *reverse annealing* in the displacement field measured by the RBS/C spectra. However, direct evidence for what precise form the free hydrogen takes is still missing. Moreover, this free H does not appear to be essential to feed the blisters, the key defects are the H-saturated platelets. PAS measurements point to large cavities ($>V_4$) as plausible sites for hydrogen retrapping. Also, by using D instead of H, we found that the degree of passivation of vacancies constitutes a critical factor in preparing the ground for blistering. The origin of the considerable isotopic differences seems to be connected with the computationally verified fact that H and D interact remarkably differently with the point defects produced during the implantation. This isotopic difference comes neither from a "magic" difference between H and D chemistries nor from an electronic effect but simply as a result of the random hopping and recombination of H/D atoms and defects. The synergistic effect observed in successive implantations of He and H ions is attributed to He assistance in accelerating the thermal evolution into passivated internal surfaces, by its significant contribution to the buildup of the pressure, required to separate internal surfaces, and by retarding the effusion of both H_2 and He. These synergistic interactions are absent for He post implantation, likely because of the dynamic destruction during implantation of the H-defect complexes that are the precursors of blisters.

ACKNOWLEDGMENTS

The authors are indebted to G. Abel and L. Andrzejewski (INRS-EMT), and Samir Elouatik (Université de Montréal) for their excellent technical work. We thank P. Nguyen for bringing to our attention Ref. 25. This research was funded by the Natural Science and Engineering Research Council of Canada and the "Fonds québécois de recherche sur la Nature et les technologie."

*Author to whom correspondence should be addressed. Present address: Max-Planck-Institut fýr Mikrostrukturphysik, Weinberg 2, D-06120 Halle, Germany. Email address: moutanab@mpi-halle.mpg.de

[1] S. J. Pearton, J. W. Corbett, and T. S. Shi, Appl. Phys. A **43**, 153 (1987).
[2] S. M. Myers *et al.*, Rev. Mod. Phys. **64**, 559 (1992).
[3] G. F. Cerofolini *et al.*, Phys. Status Solidi A **150**, 539 (1995).
[4] G. F. Cerofolini, F. Corni, S. Frabboni, C. Nobili, G. Ottaviani, and R. Tonini, Mater. Sci. Eng. **27**, 1 (2000).
[5] Chris G. Van de Walle, Phys. Rev. B **49**, 4579 (1994).
[6] Stefan K. Estreicher, Mater. Sci. Eng., R. **R14**, 319 (1995).
[7] R. Jones, B. J. Coomer, J. P. Goss, B. Hourahine, and A. Resende, Solid State Phenom. **71**, 173 (2000).
[8] E. Ligeon and A. Guivarc'h, Radiat. Eff. **27**, 129 (1976).
[9] W. K. Chu, R. H. Castle, R. F. Lever, S. Mader, and B. J. Masters, in *Ion Implantation in Semiconductors*, edited by F. Chernov, J. A. Borders, and D. K. Brice (Plenum Press, New York, 1976), p. 483.
[10] M. Bruel, Electron. Lett. **31**, 1201 (1995).
[11] S. Romani and J. H. Evans, Nucl. Instrum. Methods Phys. Res. B **44**, 313 (1990).
[12] M. Bruel, Nucl. Instrum. Methods Phys. Res. B **108**, 313 (1996).
[13] B. Aspar, H. Moriceau, E. Jalaguier, C. Lagahé, A. Soubie, B. Biasse, A. M. Papon, A. Claverie, J. Grisolia, G. Benassayag, F. Letertre, O. Rayssac, T. Barge, C. Maleville, and B. Ghyselen, J. Electron. Mater. **90**, 834 (2001).
[14] J. Grisolia, G. Ben Assayag, A. Claverie, B. Aspar, C. Lagahé, and L. Laanab, Appl. Phys. Lett. **76**, 852 (2000).
[15] Y. J. Chabal, M. K. Weldon, Y. Caudano, B. B. Stefanov, and K. Raghavachari, Physica B **273-274**, 152 (1999).
[16] S. W. Bedell and W. A. Lanford, J. Appl. Phys. **90**, 1138 (2001).
[17] T. Höchbauer, A. Misra, M. Nastasi, and J. W. Mayer, J. Appl. Phys. **89**, 5980 (2001).
[18] T. Höchbauer, A. Misra, M. Nastasi, and J. W. Mayer, J. Appl. Phys. **92**, 2335 (2002).
[19] J. K. Lee, M. Nastasi, N. D. Theodore, A. Smalley, M. Cai, and S. S. Lau, J. Appl. Phys. **96**, 280 (2004).
[20] K. K. Bourdelle, Proc.-Electrochem. Soc. **2005**, 167 (2005).
[21] O. Moutanabbir, A. Giguère, and B. Terreault, Appl. Phys. Lett. **84**, 3286 (2004).
[22] A. Agarwal, T. E. Haynes, V. C. Venezia, O. W. Holland, and D. J. Eaglesham, Appl. Phys. Lett. **72**, 1086 (1998).
[23] Xinzhong Duo, Weili Liu, Miao Zhang, Lianwei Wang, Chenglu Lin, M. Okuyama, M. Noda, Wing-Yiu Cheung, Paul K. Chu, Peigang Hu, S. X. Wang, and L. M. Wang, J. Phys. D **34**, 477 (2001).
[24] R. Tonini, F. Corni, C. Nobili, G. Ottaviani, F. Cazzaniga, and G. Queirolo, Solid State Phenom. **82**, 291 (2002).
[25] C. Lagahé-Blanchard, N. Sousbié, S. Sartori, H. Moriceau, A. Soubié, B. Aspar, P. Nguyen, and B. Blondeau, Proc.-Electrochem. Soc. **2003**, 346 (2003).
[26] Phuong Nguyen, I. Cayrefourcq, K. K. Bourdelle, A. Boussagol, E. Guiot, N. Ben Mohammed, N. Sousbie, and T. Akatsu, J. Appl. Phys. **97**, 083527 (2005).
[27] O. Moutanabbir and B. Terreault, Appl. Phys. Lett. **86**, 051906 (2005).
[28] O. Moutanabbir and B. Terreault, J. Chem. Phys. **121**, 7973 (2004).
[29] E. Bøgh, Can. J. Phys. **46**, 653 (1968).
[30] P. Asoka-Kumar, K. G. Lynn, and D. O. Welch, J. Appl. Phys. **76**, 4935 (1994).
[31] J. F. Ziegler and J. P. Biersack, SRIM-2003, www.srim.org.
[32] G. Bourque and B. Terreault, Nucl. Instrum. Methods Phys. Res. B **140**, 13–26 (1998).
[33] N. Desrosiers, A. Giguère, O. Moutanabbir, and B. Terreault, Appl. Phys. Lett. **87**, 231908 (2005).
[34] A. Uedono, T. Mori, K. Morisawa, K. Murakami, T. Ohdaira, R. Suzuki, T. Mikado, K. Ishioka, M. Kitajima, S. Hishita, H. Haneda, and I. Sakaguchi, J. Appl. Phys. **93**, 3228 (2003).
[35] M. Hakala, M. J. Puska, and R. M. Nieminen, Phys. Rev. B **57**, 7621 (1998).
[36] J. G. Swadener and M. Nastasi, Nucl. Instrum. Methods Phys. Res. B **206**, 937 (2003).
[37] R. E. Pritchard, M. J. Ashwin, J. H. Tucker, and R. C. Newman, Phys. Rev. B **57**, R15048 (1998).
[38] A. W. R. Leitch, V. Alex, and J. Weber, Phys. Rev. Lett. **81**, 421 (1998).
[39] K. Ishioka, M. Kitajima, S. Tateishi, K. Nakanoya, N. Fukata, T. Mori, K. Murakami, and S. Hishita, Phys. Rev. B **60**, 10852 (1999); T. Mori, K. Otsuka, N. Umehara, K. Ishioka, M. Kitajima, S. Hishita, and K. Murakami, Physica B **302**, 239 (2001).
[40] J. Weber, T. Fisher, E. Hieckmann, M. Hiller, and E. V. Lavrov, J. Phys.: Condens. Matter **17**, S2303 (2005).
[41] L.-J. Huang, Q.-Y. Tong, Y.-L. Chao, T.-H. Lee, T. Martini, and U. Gösele, Appl. Phys. Lett. **74**, 982 (1999).
[42] Stefano Frabboni, Phys. Rev. B **65**, 165436 (2002).
[43] N. Sousbie, L. Capello, J. Eymery, F. Rieutord, and C. Lagahé, J. Appl. Phys. **99**, 103509 (2006).
[44] P. J. Simpson, M. Vos, I. V. Mitchell, C. Wu, and P. J. Schultz, Phys. Rev. B **44**, 12180 (1991).
[45] T. Zahel, G. Otto, and G. Hobler, Proc.-Electrochem. Soc. **2005**, 179 (2005).
[46] B. Terreault, M. Chicoine, N. Desrosiers, A. Giguère, G. Hobler, O. Moutanabbir, G. G. Ross, F. Schiettekatte, P. J. Simpson, and T. Zahel, Proc.-Electrochem. Soc. **2005**, 155 (2005).